INFN Istituto Nazionale di Fisica Nucleare
LABORATORI NAZIONALI DI FRASCATI
SIS-Pubblicazioni

LNF–07/1(P)
January 1^{st}, 2007

LHC Note Project 400
April 2007

COUPLING IMPEDANCES STUDIES AND MEASUREMENTS OF THE COLDEX UPGRADED VACUUM CHAMBER

D. Alesini[1], B. Spataro[1],
M. Migliorati[2], A. Mostacci[2], L. Palumbo[2],
V. Baglin[3], B. Jenninger[3], F. Ruggiero[3]

[1)] *INFN, Laboratori Nazionali di Frascati, P.O. Box 13, I-00044 Frascati, Italy*
[2)] *University of Rome "La Sapienza", and LNF-INFN, Italy*
[3)] *CERN, Geneva, Switzerland*

Abstract

The coupling impedances of the upgraded beam screen and cold/warm transition of the cold bore experiment (COLDEX) vacuum chamber installed in the SPS machine are investigated. Detailed studies of the coupling impedances budget of the beam screen circular vacuum chamber with narrow longitudinal slots and the cold/warm transition are discussed. A comparison with the experimental tests is also presented.

Keywords: LHC, impedance, COLDEX

To be Submitted to
Nuclear Instruments & Methods in Physics Research

1 Introduction

The Large Hadron Collider (LHC) is currently under construction at CERN. The build-up of an electron cloud in the vacuum chamber might limit the LHC performance [1]. The cold bore experiment (COLDEX) is installed in the CERN SPS machine to study the interaction of the electron cloud with a vacuum system operating at cryogenic temperature. The COLDEX vacuum system houses a 2 m long perforated beam screen at 10 K inserted in a cold bore at 2 K. This experiment mimics the arc LHC vacuum system [1–3].

In an earlier paper we discussed in detail with numerical studies and experimental results the behaviour of the COLDEX vacuum chamber with elliptical cross section and pumping circular holes, in terms of the energy losses, parasitic resonances, longitudinal and transverse coupling impedances [4] [5].

The power loss was dominated by the pumping holes and estimated to be of a few tens of mW. We concluded that the observed dissipated power in COLDEX was mainly due to the electron cloud effects and could not be attributed to the coupling impedances contribution.

To reduce further the impedance of COLDEX and to increase its sensitivity to power deposition due to electron cloud, its cross section shape is changed to circular and the circular holes of the beam screen are replaced by slots. Moreover, this new geometry is closer to the LHC beam screen geometry.

The purpose of this paper is to estimate the longitudinal and transverse coupling impedances, the loss factors, produced by an array of slots in the circular coaxial vacuum chamber of the COLDEX section and in the cold/warm transition and to compare the results with the experimental ones.

The new vacuum chamber is sketched in Fig. 1. The COLDEX beam screen is in OFHC Cu with inner diameter 67 mm and 2232 mm long. The slots are 2 mm wide and 9.5 mm long with 1 mm radius at the extremity. There are 262 slots, two rows of regular periodic arrays of 131 slots uniformly spaced by 16.3 mm, in the direction of the pipe axis. In a cross-sectional view, the slots are located at -42 degrees and +42 degrees. At each extremity of the beam screen, a 0.1 mm thick stainless steel cold/warm transition is coated by 3 micron Cu and bridged at each extremity by radio frequency fingers. The middle of the cold/warm transition is thermally anchored at 80 K. The transition to the 100 mm room temperature vacuum chamber is tapered with an angle of 45 degrees.

The simulations of the cold section were carried out by using the MAFIA three-dimensional computer code [6] because of the absence of the axial rotational symmetry. The ABCI two-dimensional computer code was used for the cold/warm transition [7].

For symmetry reasons with respect to the vertical plane we simulated only half

structure to optimize the accuracy of the results which require fine mesh sizes and to minimize the CPU time requirements. Moreover, due to the mesh points limitations, the beam screen and the cold/warm transition were treated separately. The geometries for the simulations are reported in Figs. 2 and 3, respectively.

The calculations have been made by supposing OFHC copper structures with a conductivity of 5.91×10^7 $(\Omega\ \mathrm{m})^{-1}$ at room temperature. We also assume that the bunches in the SPS machine are arranged in 4 batches separated by 225 ns, each containing 72 bunches. The bunch spacing is 25 ns, the r.m.s./ bunch length is approximately 0.2 - 0.25 m and the nominal bunch population is about 1.15×10^{11} protons. Since the losses are very small, in order to estimate the longitudinal loss parameter accurately and to avoid intrinsic numerical noise, we simulated a shorter bunch length of 0.12 m.

2 Beam screen numerical studies

Several papers have been devoted to the study of the effects, on beam dynamics, of pumping holes coupling of the vacuum chamber to an external antichamber.

The design of the shape and the position of the perforations (hole, slot, etc) has to meet several conflicting requirements. These requirements include the minimizing of the beam coupling impedance but ensuring a sufficient pumping speed.

It is well known that the electromagnetic interaction between a particle and the accelerator pipe wall is described by two frequency dependent parameters: the longitudinal and transverse coupling impedances or the corresponding wake potentials.

For wavelengths larger than the hole size, the coupling impedance can be calculated in terms of electric and magnetic polarizabilities of the hole which are geometrical factors at the low frequencies regime [8,9]. The important predictions of this theory allow to optimize the shape of the holes in order to minimize the impedance contribution [4,10]. Of great importance is a hole of a rectangular shape, similar to the shape of the pumping slots in a beam screen. The impedance of narrow rectangular slots oriented in the direction of the pipe axis is mostly influenced by the width and shape of the ends of the slots and it does not depend on the length of the slots [11–13]. Increasing the slot length can also bring resonances due to the slot length to low frequencies [14]. However, at very low frequency, usually the imaginary part of the impedance is the main contribution since it is much larger than the real part.

At higher frequencies this procedure can be no longer followed because the static approximation loses its validity in case that the slot length becomes comparable with the wavelengts contained in the beam spectrum lines.

Based on this analysis, we therefore expect that a regular array of identical narrow

slots distributed along the longitudinal axis are the best choice for pumping holes since it produces a low impedance for a finite hole area. We will also extend the study to examine the behaviour of possible resonant effects in the slots.

Our main goal is to apply such procedure to perform a detailed study to minimize the coupling impedances and reduce the heating of the beam screen reported in Fig. 2.

The vacuum chamber has a circular constant cross section. The slots sizes are smaller with respect to the wavelengths of the bunch spectrum lines during the SPS machine operation. Quantitative estimations of both longitudinal and transverse coupling impedance, parasitic resonances and energy losses, produced by an array of N slots in the chamber walls in the beam screen have been performed with MAFIA simulations in the time domain.

In order to study the behaviour of the real structure, detailed simulations have been performed also with 30 and 132 slots (total of two rows).

3 Beam screen longitudinal and transverse loss factors behaviour for 30 slots (total of two rows)

The beam - vacuum chamber coupling impedance and the power losses do not depend linearly on the beam position inside the chamber for structures having no rotational symmetry.

In order to get a deeper insight of the involved physics because of the asymmetry (Fig. 2), the longitudinal and the transverse loss parameters [4] estimations as function of the off-axis beam displacement along the vertical coordinate (cross-section symmetry plane) of the COLDEX section with an array of 30 slots (15 slots per row) have been carried out.

To evaluate the short range wake potential over the bunch length, a single Gaussian bunch with s = 0.01 m has been considered. The corresponding results are shown in Fig. 4, where the loss parameters are normalized to their maximum values.

One observes that the longitudinal and transverse loss parameters are function of the beam position inside the chamber with an asymmetric distribution along the vertical plane as it is expected to be. Such behaviour is physically sound since the electromagnetic field is obviously much more perturbed in the slots region (negative coordinates).

The longitudinal loss parameter is maximum at about y = -0.014 m with respect to the centre of the reference system shown in Figs. 2 and 4. It is also noted that the transverse loss factor is proportional to the derivative of the longitudinal one as the Panofsky - Wenzel theorem states for coupling impedances. As a result, its maximum value is obtained at about y = -0.024 m, nearer to the chamber wall.

4 Case with 132 slots (total of two rows)

For obtaining a realistic estimation of the coupling impedances, for a σ = 0.12 m bunch length and with 132 slots (total of two rows), we report in Table 1 the longitudinal loss factor, power losses, equivalent longitudinal inductance L and absolute maximum value of the longitudinal wake potential $|W_{max}|$ of the structure of Fig. 1; and in Table 2 the transverse loss parameter and impedance, as a function of some relevant beam positions in the beam screen of the same structure. The Z/n value has been obtained from the pure imaginary impedance.

Slots number (total of two rows)	Vertical position (m)	$\|W_{max}\|$ $\times 10^7$ (V/C)	L (pH)	Z/n $(\mu\Omega)$	Long. loss factor (V/C)	Power losses (μ W)
132	0.0	5.0	33	9.0	185	.80
132	-0.014	10	66.5	18.2	272	1.17
132	-0.024	5.1	33.1	9.0	97	0.42

Table 1: Longitudinal impedances and power losses.

Slots number (total of two rows)	Vertical position (m)	Transverse loss factor $\times 10^8$ (V/C)	Transverse impedance (Ω)
132	0.0	-2.9	0.41
132	-0.014	-0.072	+0.01
132	-0.024	+5.8	-0.82

Table 2: Transverse impedances.

The average power P lost by the beam is calculated with the relation [4]:

$$P = K_l N_b I^2 T \tag{1}$$

with K_l the longitudinal loss factors, N_b the number of bunches circulating in the ring, I the average current per bunch and T the revolution time; the equivalent longitudinal inductance is given by the theoretical relation [15],

$$|W_{max}| = \frac{Lc^2}{\sqrt{2e\pi}\sigma^2} \tag{2}$$

with e the Neper number and $|W_{max}|$ the wake potential maximum or minumum value; the transverse impedance is given by the analytical model [16]

$$Im[Z(f=0)] = -2\sqrt{\pi}K_t\frac{\sigma}{c} \tag{3}$$

with K_t the transverse loss factor.

As an example we illustrate in Fig. 5 the wake potential (normalized to its maximum value): the impedance is purely inductive at the geometric centre of the vacuum chamber.

To completely characterize the section with 132 slots (66 per row), the longitudinal long range wake potential has been simulated by assuming a smaller bunch length with σ = 0.01 m over a distance of 2 meters. Then, the coupling impedance has been calculated by the Fourier transform of the wake-potential.

The cut-off frequencies of the vacuum chamber have been estimated to be 2.62 GHz for the TE mode and 3.43 GHz for the TM one.

The simulations were carried out for some values of beam position along the vertical coordinate.

There are two potential sources of parasitic resonances due to the slots at high frequencies related to the distribution and the length of the slots [14,17]. In general, these peaks can be reduced by randomization of the longitudinal displacements of the slots positions. In all cases no specific problem was found to be in the frequency range of concern for the SPS operation bunch spectrum lines.

As an example, here we report the case with the beam position at the vacuum chamber centre and where the longitudinal and transverse loss factors assume the maximum values.

The longitudinal real and imaginary part of the coupling impedance are reported in Figs. 6 and 7 in case of the beam position is located at the centre of the chamber and at the vertical coordinate at y = -0.014 m (corresponding to the maximum longitudinal loss factor).

The transverse case is shown in Fig. 8 when the beam position is located at the centre of the chamber. Also in this case the $Im[Z(f=0)]$ = 0.41 Ω is in an excellent agreement with the previous results of the table 2.

From the Figs. 6 and 7 one can see the presence of parasitic resonances and that the first one occurs at a frequency f = 9.5 GHz very far from the bunch relevant spectrum lines (the beam cut - off frequency is about 400 MHz); the peaks magnitude depends on the beam position according to the loss factor behaviour in Fig. 4.

The imaginary impedance up to 7 GHz is about a linear function of the frequency, thus giving an inductive behaviour. The total inductance of 132 slots (66 per row) is given by L = 32.87 pH at the centre of the chamber confirming the value reported in table 1.

The reported results give interesting ideas for the final design of the structure. We believe that the nominal slots number section of design with 264 slots (132 per row) will also give no specific problem since it will follow the same behaviour than the structure already examined with 132 slots (66 per row).

5 Whole beam screen section studies

As shown in the previous sections, since the bunch length is longer than the distance between the slots, the narrow peaks of the parasitic resonances are outside the relevant bunch spectrum lines, and at low frequency the coupling impedance imaginary part dominates the real one[1]. During the machine operation, the maximum beam offset is expected to be few mm [18].

In order to investigate the behaviour of the whole cold bore transition, we calculated the longitudinal and transverse loss parameters, the equivalent inductance, as function of the slots number N by assuming a Gaussian bunch length with σ = 0.12 m.

Theoretical studies [19] for a large slots number N, with a bunch length greater than the distance between the slots and for a large number of them and in presence of ohmic losses, show that the longitudinal loss factor grows approximately quadratically for a small slots number N, while it grows linearly for large N.

Figs. 9 and 10 show the fits of the longitudinal and transverse loss factors respectively with the beam position at the centre of the chamber. These figures clearly show the linear fit dependences as function of the slots number N.

The numerical results are in agreement with the theoretical predictions [19] where the linear term dominates the quadratic one for small slots number.

As a conclusion, at the vacuum chamber centre, for the whole section with a slots number N = 264 (total of two rows), we get a longitudinal loss parameter around at K_l = 350 V/Q resulting to a power loss P = 1.5 μW. Assuming about 2.2 m structure we obtain 0.7 μW/m. In the worst case scenario of a beam displacement of 1 cm the power loss is approximately 3 μW (1.33 μW/m).

From Fig. 10, the transverse loss parameters scales exactly with the slots number N according the theoretical model. As far as the transverse impedance calculations and applying the relation (3), the imaginary part of the transverse impedance is estimated to be about $Im[Z(f = 0)]$ = 0.82 Ω.

In Fig. 11 the fits of the equivalent inductance for two beam position are reported: vacuum chamber centre and $x = 0$ m, $y = -0.014$ m. Again, the two equivalent inductances L go linearly with the slots number N according to the analytical model as

[1]The loss factors shown before include the ohmic losses

expected (for example see [4,10,11,13]). Again we find that the inductance increases two times faster at $x = 0$ m, $y = -0.014$ m than in the vacuum chamber centre. At the vacuum chamber centre we get L = 66 pH by giving a longitudinal broaband impedance Z/n = 18 $\mu\Omega$.

6 Cold/warm transition

The cold/warm transition is a tapered vacuum chamber that goes from a diameter of 67 mm to another one of 100 mm with an angle of 45 degree (Fig. 3). Also in this section, no specific problem was found in the frequency range of concern for the SPS operation bunch spectrum lines. Calculations on this section have been carried out by using the ABCI code [7] and an analytical approach [20]. As a result, the longitudinal impedance is estimated to be Z/n = 0.37 mΩ and the transverse one Z = 485 Ω/m, while the loss factor is 2.8$\times 10^7$ V/C. At each extremity of the COLDEX beam screen one of such cold/warm transition is installed [3]. For symmetry reasons, the resulting power loss is negligible [21].

7 Experimental results

Fig. 12 shows the dissipated power per unit length in the COLDEX as a function of the SPS bunch current [22]. The measurements are done when 4 batches of 72 bunches are circulating in the SPS. The beam screen operates at 12 K and the cold bore at 3 K. This intensity scan shows a threshold at 7×10^{10} protons/bunch in agreement whith the appearance of an electron cloud inside the beam screen. In the meantime, a pressure increase due to the electron bombardment of the beam screen wall was observed but is not shown here. Above the threshold, the dissipated heat increases linearly with the bunch current. At 1.15×10^{11} protons/bunch, the dissipated power is about 0.9 W/m in the whole beam screen section. This value exceed by a factor 10^6 the estimated parasitic loss due to the coupling impedance of the structure with the beam. Therefore the contribution of the power loss due to impedance is negligible with respect to the dissipated power onto the COLDEX beam screen.

8 Conclusions

In this paper we have discussed the power dissipated in the COLDEX upgraded vacuum chamber due to ohmic losses and pumping holes.

As expected, due to the choice of the circular pumping holes, the power loss on the COLDEX vacuum chamber has been reduced from 0.4 mW [4] to the actual 1.5 μW.

Coupling impedance and loss factor have been computed numerically and the results checked against theoretical predictions. The power loss due to pumping holes is expected to be few orders of magnitudes smaller than the power dissipated because of electron cloud. Also the coupling impedances are negligible.

References

[1] ”LHC Design report” edited by O. Brning et al. CERN-2004-003 4 June 2004. CERN Geneva, Switzerland.

[2] V. Baglin, I. R. Collins, B. Jenninger, ”Performances of a Cryogenic Vacuum System (COLDEX) with an LHC Type Beam”, Vacuum 73 (2004) 201-206.

[3] V. Baglin, B. Jenninger, ”Pressure and Heat Load in a LHC type Cryogenic Vacuum System Subjected to Electron CLOUD”, Proceedings of the 31st Advanced ICFA Beam Dynamics Workshop on Electron-Cloud Effects, Ecloud04, Napa, California, 19-23 April 2004; also CERN-2005-001 12 January 2005. CERN Geneva, Switzerland.

[4] B. Spataro, D. Alesini, M. Migliorati, A. Mostacci, L. Palumbo, F. Ruggiero, ”Cold to warm transition impedances in the SPS machine”, First CARE-HHH-APD Workshop, Geneve, 8-11 November 2004;

[5] B. Spataro, D. Alesini, M. Migliorati, A. Mostacci, L. Palumbo, F. Ruggiero, ”Impedances of the cold bore experiment, COLDEX, installed in the SPS machine”, NIM A 564 (2006) pp. 38-43;

[6] R. Klatt et al., ”MAFIA - a three dimensional electromagnetic CAD system for magnets, RF structures and transient wake-field calculations. Proceedings of the 1986 Linear Conference, Stanford Linear Accelerator Center, SLAC - Report 303,June 1986 (pp. 276-278) or http://www.cst.com;

[7] Y.H. Chin, CERN LEP-TH/88-3 (1988);

[8] S.S. Kurennoy,” Coupling impedance of pumping holes”, Part. Acc. Vol. 39, 1 (1192);

[9] S. De Santis, M. Migliorati, L. Palumbo and M. Zobov, Phys. Rev. E 54, 800 (1996);

[10] R. L. Gluckstern, Phys . Rev. A 46, 1110 (1992);

[11] S. S. Kurennoy, ”Pumping slots, coupling impedance calculations and estimates”, Technical Report SSCL-636,SSCL, 1993;

[12] G.V. Stupakov, ”Coupling impedance of a long slot and an array of slots in a circular vacuum chamber”, Phy Rev. E vol. 51, 4 (1995);

[13] S. De Santis, A. Mostacci, L. Palumbo, B. Spataro, ”Analytical expressions for the coupling impedance of a narrow slot in a coaxial beam pipe”, Phys. Rev. E vol. 58, n.5 (1998);

[14] R. L. Gluckstern, ”Coupling impedance of many holes in a liner within a beam pipe”, Phy. Rev. A, 46:1110, 1992;

[15] S. Bartalucci, M. Serio, B. Spataro, M. Zobov,” Broad-band model impedance for DAFNE main rings”,NIM A 337 (1994)231-241;

[16] G.V. Stupakov,” Geometrical wake of a smooth taper”, SLAC-PUB-95-7086, Dec. 1995;

[17] S. S. Kurennoy, ”Trapped modes in waveguides with small discontinuity”, Phys. Rev. E vol 51, 2498 (1995);

[18] G. Arduini, private comunications;

[19] A. Mostacci, L. Palumbo, F. Ruggiero, ”Impedance and loss factor of a coaxial liner with many holes: effect of the attenuation”, Phys. Rev. Spec. Topics A&B, vol. 5, 044401, (2002);

[20] K.Yokoya,”Impedance of slowly Tapered Structures, Tech. Rep. SL/90-88 (AP), CERN (1990);

[21] L. Palumbo, V. G. Vaccaro, and M. Zobov, ”Wake Fields and Impedance”, LNF - 94 / 041 (P), 3 September 1994.

[22] V.Baglin, ”Latest results from COLDEX (Pressure, Heat load, Ion production)”, presented at the 47th Accelerator Performance Committee 26th May 2005. http://ab-div.web.cern.ch/ab-div/Meetings/APC/2005/apc050526/V_Baglin_slides.pdf;

Figure caption

Figure 1: Sketch of half of the COLDEX section vacuum chamber. The left and right pictures represent the beam screen and cold to warm transition respectively.

Figure 2: Shape of the beam screen used for MAFIA simulations.

Figure 3: Shape of the cold to warm transition for ABCI simulations.

Figure 4: Nomalized longitudinal and transverse loss factor as function of the verical beam displacement for N=30 slots (total of two rows).

Figure 5: Normalized longitudinal wake potential for 132 slots (total of two rows) at the geomtetric centre of vacuum chamber (x=y=0) with $|W_{max}|$ = 5×10^7 V/C.

Figure 6: Real longitudinal coupling impedance for 132 slots (total of two rows) at x=0 and y=0 (dots) and y=-0.014 m (solid) of the COLDEX section estimated by using the wake potential Fourier transform.

Figure 7: Imaginary longitudinal coupling impedance for 132 slots (total of two rows) at x=0 and y=0 (dots) and y=-0.014 m (solid) of the COLDEX section estimated by using the wake potential Fourier transform.

Figure 8: Real and imaginary transverse coupling impedance for 132 slots (total of two rows) at the geometric centre of the COLDEX section estimated by using the wake potential Fourier transform.

Figure 9: Fit of the longitudinal loss parameter as function on the slots number N calculated at the centre of vacuum chamber.

Figure 10: Fit of the transverse loss parameter as function on the slots number N calculated at the centre of vacuum chamber.

Figure 11: Fit of the equivalent inductance L as function of the slots number N calculated at the beam position x=y=0 (circle) and x=0, y=-0.014 m (square). x=y=0 is the vacuum chamber centre.

Figure 12: Power dissipated onto the COLDEX beam screen per unit length as a function of the bunch current when 4 batches of 72 bunches circulate in the SPS.

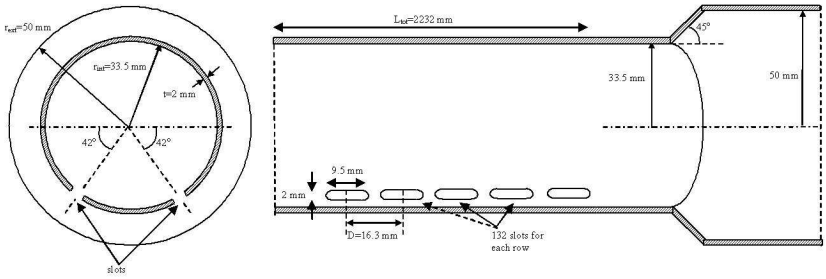

Figure 1: Sketch of half of the COLDEX section vacuum chamber. The left and right pictures represent the beam screen and cold to warm transition respectively.

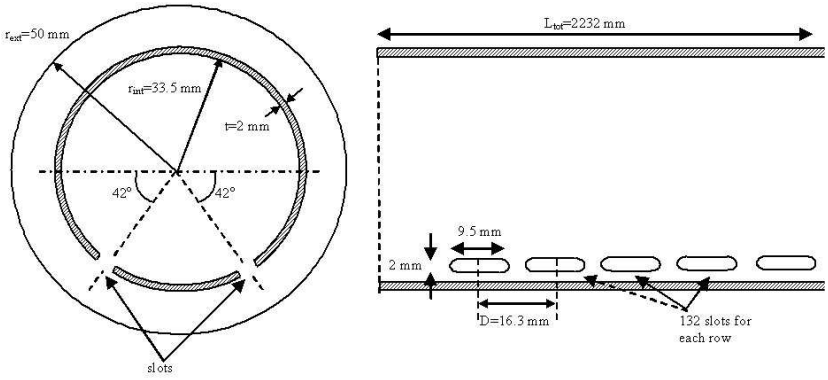

Figure 2: Shape of the beam screen used for MAFIA simulations.

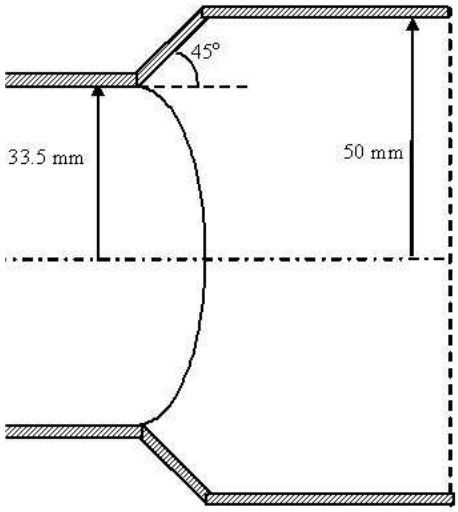

Figure 3: Shape of the cold to warm transition for ABCI simulations.

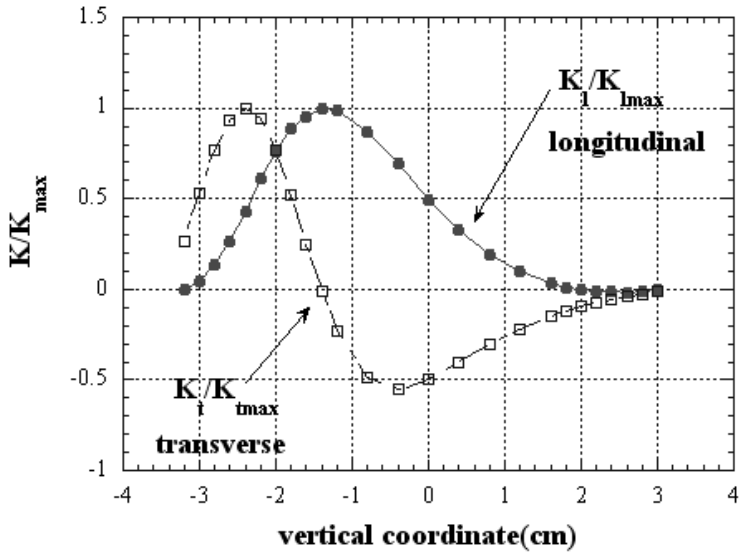

Figure 4: Nomalized longitudinal and transverse loss factor as function of the verical beam displacement for N=30 slots (total of two rows).

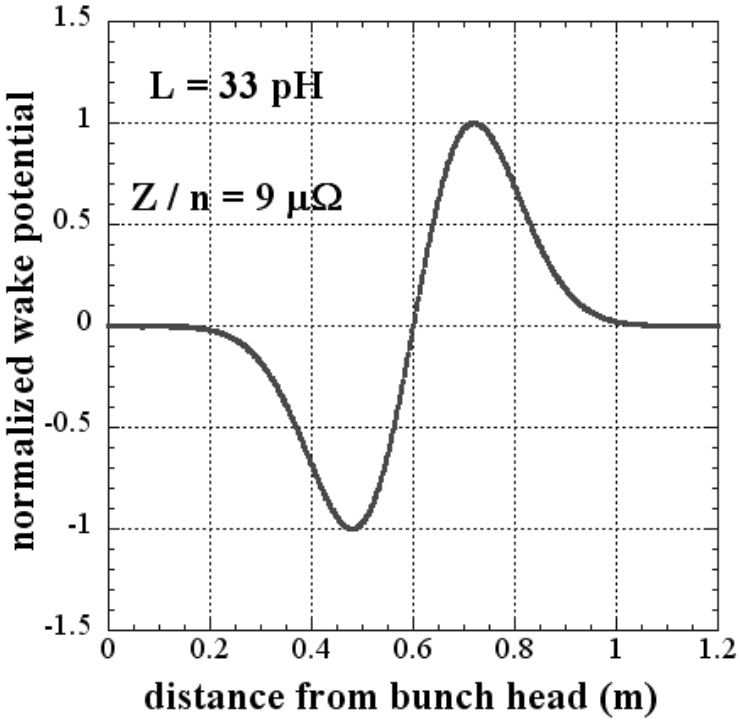

Figure 5: Normalized longitudinal wake potential for 132 slots (total of two rows) at the geomtetric centre of vacuum chamber (x=y=0) with $|W_{max}|$ = 5×10^{7} V/C.

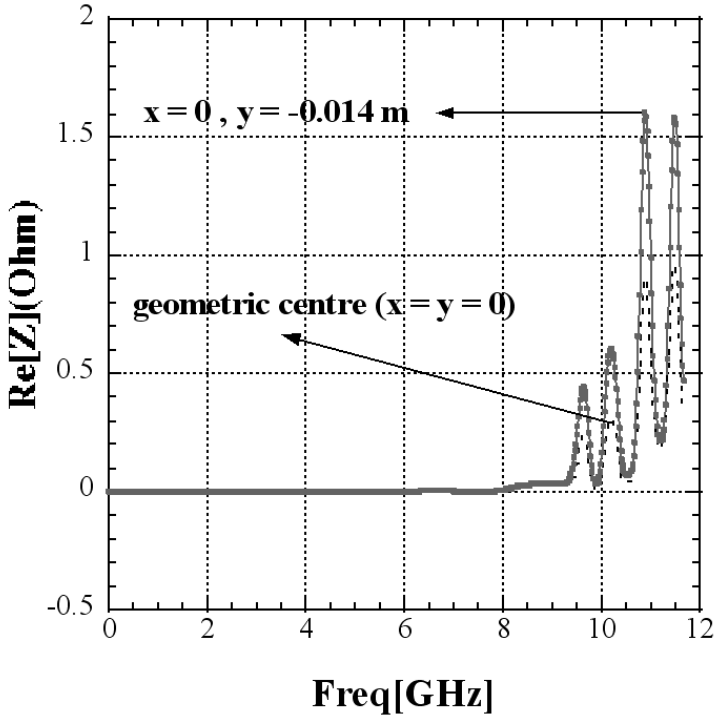

Figure 6: Real longitudinal coupling impedance for 132 slots (total of two rows) at x=0 and y=0 (dots) and y=-0.014 m (solid) of the COLDEX section estimated by using the wake potential Fourier transform.

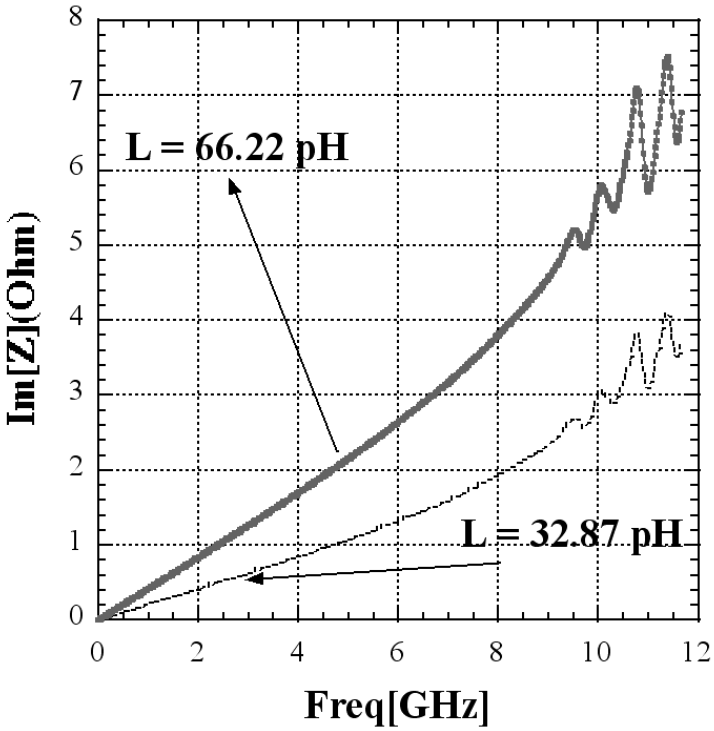

Figure 7: Imaginary longitudinal coupling impedance for 132 slots (total of two rows) at x=0 and y=0 (dots) and y=-0.014 m (solid) of the COLDEX section estimated by using the wake potential Fourier transform.

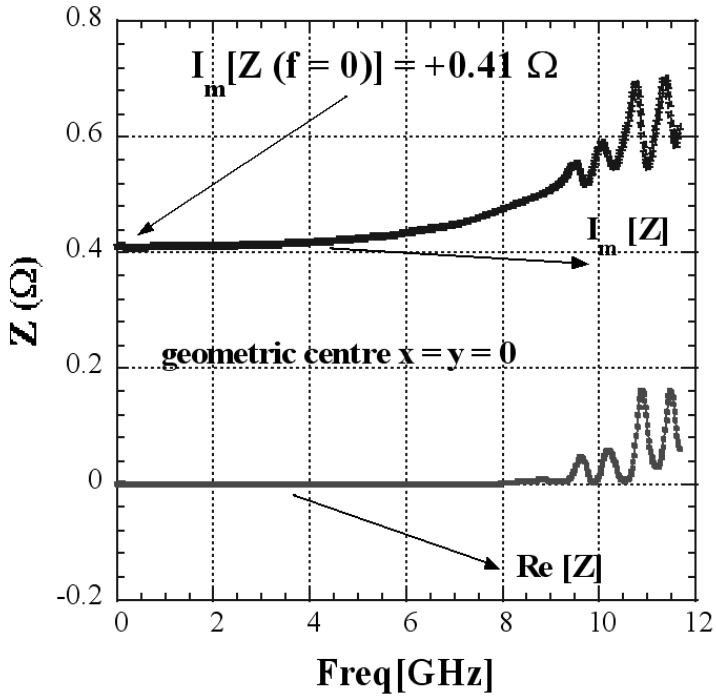

Figure 8: Real and imaginary transverse coupling impedance for 132 slots (total of two rows) at the geometric centre of the COLDEX section estimated by using the wake potential Fourier transform.

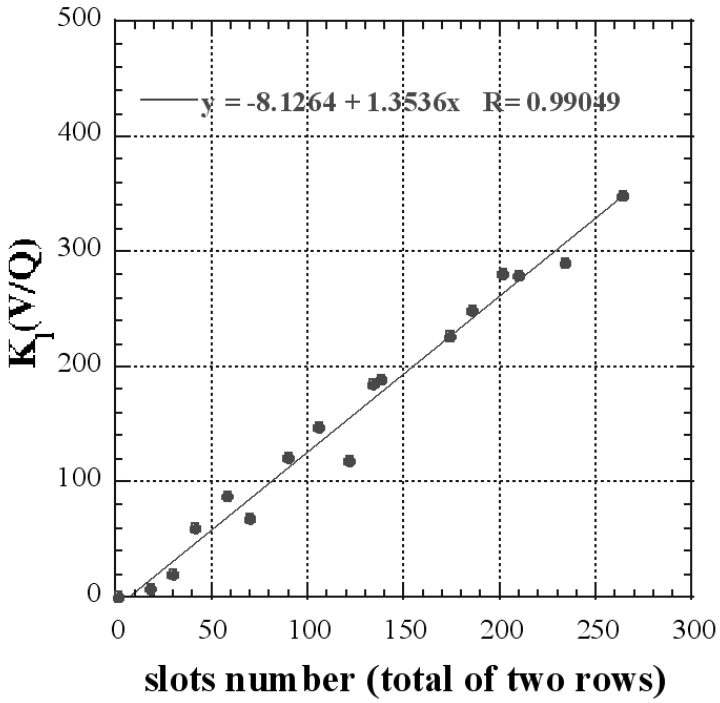

Figure 9: Fit of the longitudinal loss parameter as function on the slots number N calculated at the centre of vacuum chamber.

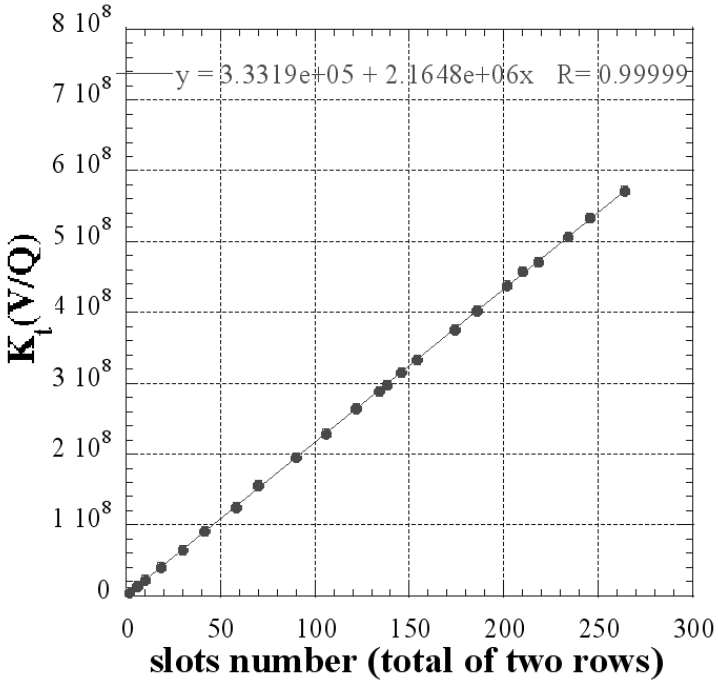

Figure 10: Fit of the transverse loss parameter as function on the slots number N calculated at the centre of vacuum chamber.

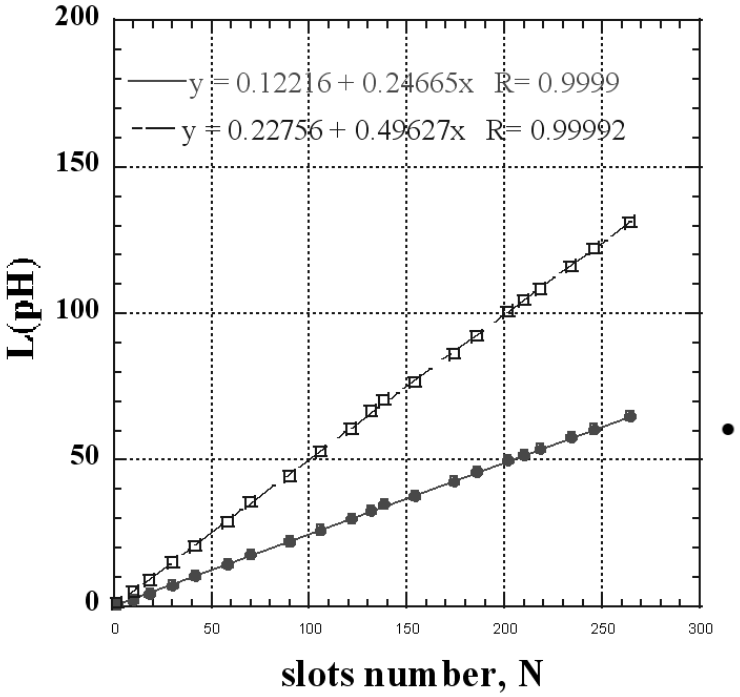

Figure 11: Fit of the equivalent inductance L as function of the slots number N calculated at the beam position x=y=0 (circle) and x=0, y=-0.014 m (square). x=y=0 is the vacuum chamber centre.

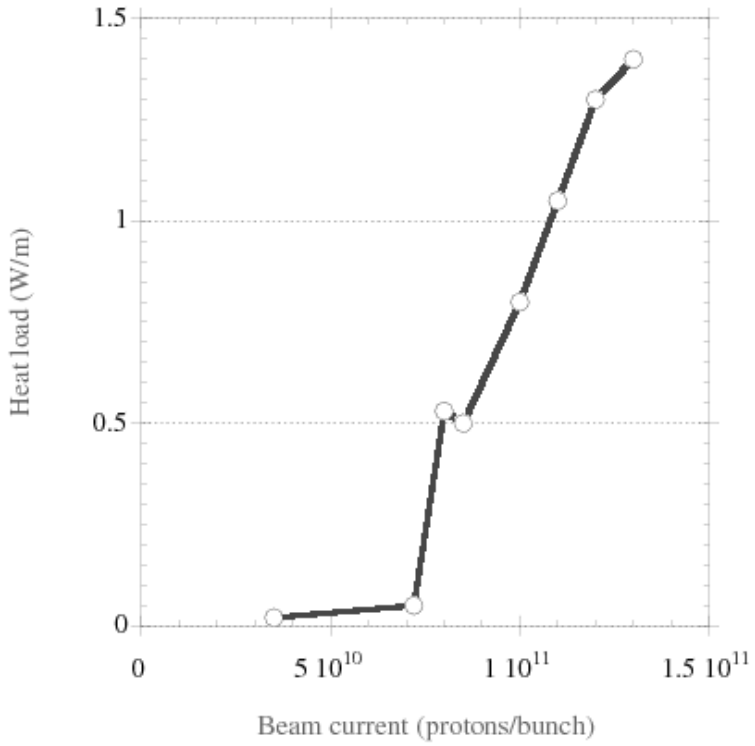

Figure 12: Power dissipated onto the COLDEX beam screen per unit lenth as a function of the bunch current when 4 batches of 72 bunches circulate in the SPS.